

3. Calculate $\frac{\partial H}{\partial u_k}$, $\frac{\partial H_1}{\partial v_i}$, $\frac{\partial H_2}{\partial w_j}$ and make a correction in the control given by*

$$\delta u_k = \epsilon \frac{\partial H}{\partial u_k} \quad (\text{IIa})$$

$$\delta v_i = \epsilon \frac{\partial H_1}{\partial v_i} \quad (\text{IIb})$$

$$\delta w_j = \epsilon \frac{\partial H_2}{\partial w_j} \quad (\text{IIc})$$

Notice that from Equation (Ig), this guarantees δI increasing with each iteration if ϵ is picked small enough.

4. Integrate the state equations and get a new value of I .

5. If $I > \bar{I}$ (a success), then double ϵ , and go back to (3). If $I < \bar{I}$ (a failure), then divide ϵ by 4 and go back to (3). If after at least one success, we get a failure, then fit a quadratic in ϵ to I to find the optimal ϵ in the direction given

by (IIa) to (IIc). Then go back to (2).

6. Terminate the procedure when it is felt the optimum has been reached. This method has been found to be more efficient than simple steepest ascent, and it has the property that constraints of the type in Equation (10) are no problem. When a constraint is reached, it is followed and the basic properties of the algorithm are unchanged.

Conjugate Gradient Method. This method, based on the ideas of Fletcher and Reeves (24) for discrete systems, has been developed for lumped parameter optimization by Lasdon *et al.* (25). As in the case of discrete systems, a requirement for the method to work is that the controls be unconstrained. Our use was therefore limited to the steps in the iteration where the controls remained unconstrained. In these cases the method was noticeably more efficient than the modified gradient method. Our application of it was for the adiabatic reactor examples where v_i and w_j were fixed in advance, in which case the method is identical to that described by Lasdon *et al.* (25).

* These corrections will be modified if u_k is a function of only one independent variable or if v_i and w_j are constants as discussed in Appendix I.

Heat and Mass Transfer in the Wall Region of Turbulent Pipe Flow

G. A. HUGHMARK

Ethyl Corporation, Baton Rouge, Louisiana

Models for the laminar sublayer of turbulent pipe flow are reviewed. The observations of the sublayer by Popovich and Hummel and the experimental fluctuation frequencies obtained by Shaw and Hanratty are used with the models to evaluate experimental heat and mass transfer data. The eddy diffusivity model and a parallel conductance model appear to be consistent with the experimental data.

Heat and mass transfer in the wall region for turbulent flow has been a subject of continuing interest. Several models have been proposed to represent the rate of transport from the wall to a turbulent fluid. These must obviously represent the behavior of the fluid in the immediate vicinity of the wall. The fluid velocity increases from a very small value near the wall to a large value for the region of free turbulence in the core. A thin nonturbulent layer has been postulated next to the wall which has been designated as the laminar sublayer. The mechanism of momentum, heat, and mass transport would thus be molecular rather than by eddy motion. Fage and Townend (1) examined the motion of small dust particles in water under the ultramicroscope very near the wall and found no evi-

dence of the existence of a region possessing rectilinear motion. Lin *et al.* (2) obtained data for concentration profiles with mass transfer at Schmidt numbers of about 900 and concluded that there is no laminar film corresponding to molecular diffusion. Subsequent mass transfer data have been obtained at Schmidt numbers up to 100,000, and these data show that the observed rate is much greater than could occur with a fully developed laminar film and molecular diffusion at the pipe wall. Popovich and Hummel (3) have used a flash photolysis method to study the wall region for turbulent flow in a square smooth pipe at a Reynolds number of 13,100. This work shows that there is a layer $y^+ = 1.6 \pm 0.4$ in which there is always a linear velocity gradient but the slope of

the gradient changes with time. A broadened trace was observed at the wall in approximately 45% of the observations. The statistical distribution curve of the thickness of the laminar sublayer showed that the most probable thickness is $y^+ = 4.3$ and the average thickness is $y^+ = 6.17$. Turbulence was observed at all times beyond $y^+ = 34.6$.

The objective of this paper is to analyze the models for transport in the wall region with respect to the observations of Popovich and Hummel and available experimental data for heat and mass transfer.

LAMINAR SUBLAYER MODELS

Several different models have been used to represent this laminar sublayer after it became apparent that this region could not be represented as fully developed laminar flow. The eddy diffusivity concept has been one of the most generally used methods (2, 4). This utilizes an equation of the form

$$\frac{\epsilon}{\nu} = a(y^+)^n \quad (1)$$

to represent experimental mass transfer data obtained for fully developed turbulent flow at large Schmidt numbers. The eddy viscosity concept has also been applied by differentiation of experimental velocity profile data. Sherwood, Smith, and Fowles (5) have used this method with the assumption that the turbulent Prandtl and Schmidt numbers are not unity in the wall region in order to fit experimental transfer data. The penetration theory and combinations of the film and penetration theory have also been used. In its simplest form, eddies are assumed to be in direct contact with the wall, and the equation

$$k = 2 \sqrt{\frac{D}{\pi \theta}} \quad (2)$$

is applicable. Harriott (6) proposed a combination of the film and penetration theories to represent a fully developed laminar region between the wall and the eddies.

$$\frac{1}{k} = \frac{\delta}{D} + \frac{1}{2 \sqrt{\frac{D}{\pi \theta}}} \quad (3)$$

Marchello and Toor (7) also used a combination of the two theories but assumed that localized mixing rather than gross fluid displacement occurs at the low turbulence levels near a wall and that transport is by molecular diffusion between mixing. This is represented by

$$\frac{\epsilon}{D} = \sqrt{\frac{\beta}{D}} \frac{1 + \cosh 2\sqrt{\beta/D}}{\sinh 2\sqrt{\beta/D}} - 1 \quad (4)$$

β is a turbulence parameter given by

$$\beta = S\tau^2 \quad (5)$$

Hughmark (8) proposed a parallel conductance model for the boundary layer

$$k = k_L + 2 \sqrt{\frac{D}{\pi \theta}} \quad (6)$$

to represent the contribution of laminar and eddy mass transfer. Analysis of experimental heat and mass transfer data with the eddy frequency data of Shaw and Hanratty (9) indicated an effective laminar layer thickness of $y^+ = 0.45$.

The observations of Popovich and Hummel are useful in evaluating the models. This work indicates that

1. A region of essentially linear velocity gradient exists at the wall.

2. The laminar sublayer shows characteristic laminar traces but with periodic changes of slope of the velocity profile.

3. The traces in the laminar sublayer show periodic broadening all the way to the wall. These conclusions indicate that laminar flow does exist in this sublayer but that fluid elements do enter the layer which results in the observed broadening of the traces. Also the changes in slope of the velocity profile indicate that the flow is not of a fully developed laminar nature. The various models can then be analyzed with respect to these observations.

Equations (2) and (3) can be eliminated from consideration as models of the laminar sublayer. Equation (2) is not applicable because a region of essentially linear velocity gradient appears to exist at the wall. Equation (2) requires a response of $k \sim D^{0.5}$. Experimental data for mass transfer at high Schmidt numbers show $k \sim D^{0.62}$, which is another indication that Equation (2) is not applicable. Equation (3) represents a fully developed laminar layer at the wall. This model is not consistent with the observations of Popovich and Hummel. Equations (1), (4), and (6) remain to be evaluated with respect to the experimental data for heat and mass transfer.

EDDY DIFFUSIVITY MODEL

The Popovich and Hummel work indicates the alternate presence of laminar and eddy conditions in the laminar sublayer. The eddy diffusivity model represented by Equation (1) can be used if this diffusivity represents a time average of the laminar and eddy conditions. Son and Hanratty (4) have developed this model, and the data of Harriott and Hamilton (10) have been used (11) to determine the equation

$$k_E = 0.0816 u^* (N_{Sc})^{-2/3} \quad (7)$$

This equation represents experimental data for a 0.94-in. diam. pipe with a Schmidt number range of 6,000 to 100,000. Data obtained by Kishinevsky, Denisova, and Parmenov (12) for a 0.51-in. diam. pipe result in the equation

$$k_E = 0.078 u^* (N_{Sc})^{-7/12} \quad (8)$$

for the Schmidt number range of 6,000 to 31,000. These results indicate different eddy diffusivity relationships for the two pipe sizes

$$\frac{\epsilon}{\nu} = 0.00096 y^{+3} \quad (9)$$

for the 0.94-in. pipe and

$$\frac{\epsilon}{\nu} = 0.0045 y^{+2.4} \quad (10)$$

for the 0.51-in. pipe. Equations (9) and (10) are obviously greatly different and raise a question as to a diameter effect on the eddy diffusivity model.

Experimental heat transfer data are available for a range of pipe diameters with Prandtl numbers to 370. These data can be useful in evaluating the eddy diffusivity model if the heat transfer in the laminar sublayer can be isolated. This requires a model for heat and mass transfer in the transition region based upon the velocity profile and the total diffusivities for this region.

WALL REGION VELOCITY PROFILE

Hanratty (13) proposed an analysis for the wall region based upon the turbulent exchange of mass and momentum

with the wall. To obtain the velocity profile, he assumed that

1. The wall exchange process on the average can be represented by the motion of masses of fluid possessing a fixed velocity u_L and a fixed wall-contact time θ_c .

2. The transport of momentum within any one of these masses can be represented by the equation

$$\frac{\partial u}{\partial \theta} = \frac{\mu}{\rho} \left(\frac{\partial^2 u}{\partial y^2} \right) \quad (11)$$

Hanratty used the boundary conditions

$$\begin{aligned} y = 0 & & u = 0 \\ y = \infty & & u = u_L \\ \theta = 0 & & u = u_L \end{aligned}$$

and solved Equation (11) to obtain the velocity corresponding to the time θ

$$u = u_L \operatorname{erf} \left(\frac{y}{2 \sqrt{\frac{\mu}{\rho} \theta}} \right) \quad (12)$$

and used the penetration theory model for the instantaneous rate of momentum transfer to the wall:

$$\tau_0 g_c = \rho u_L \sqrt{\frac{\mu}{\rho \pi \theta}} \quad (13)$$

Equations (12) and (13) were integrated to represent the averaging effect of all masses in contact with the wall and these equations were then combined to obtain the equation

$$u^+ = u_L^+ \int_0^1 \operatorname{erf} \left(\frac{y^+ \sqrt{\pi}}{4 u_L^+ \sqrt{\theta/\theta_c}} \right) d \left(\frac{\theta}{\theta_c} \right) \quad (14)$$

Hanratty assumed that u_L^+ corresponds to the break point between the turbulent core and the buffer layer. Thus he used values of $y^+ = 30$ and $u_L^+ = 13.5$. The velocity profile obtained from Equation (14) and $u_L = 13.5$ provided a satisfactory representation of experimental velocity profile data. As pointed out by Hanratty, this expression would be expected to hold only for y^+ much less than 30 because of the boundary conditions. This objection can be eliminated by selection of the boundary conditions:

$$\begin{aligned} y = 0 & & u = 0 \\ y = y_L & & u = u_L \\ \theta = 0 & & u = u_L \end{aligned}$$

Solution of Equation (11) with these boundary conditions yields

$$u = u_L \sum_{K=0}^{K=\infty} \left\{ \operatorname{erf} \left[\frac{(2K+1)(y_L) + (y_L - y)}{2 \sqrt{\frac{\mu}{\rho} \theta}} \right] - \operatorname{erf} \left[\frac{(2K+1)(y_L) - (y_L - y)}{2 \sqrt{\frac{\mu}{\rho} \theta}} \right] \right\} \quad (15)$$

Equations (13) and (15) can be integrated and combined in a manner similar to that used by Hanratty to obtain the equation

$$u^+ = u_L^+ \int_0^1 \left\{ \operatorname{erf} \left[\frac{(2K+1)(y_L^+) + (y_L^+ - y^+) \sqrt{\pi}}{4 u_L^+ \sqrt{\theta/\theta_c}} \right] - \operatorname{erf} \left[\frac{(2K+1)(y_L^+) - (y_L^+ - y^+) \sqrt{\pi}}{4 u_L^+ \sqrt{\theta/\theta_c}} \right] \right\} d \left(\frac{\theta}{\theta_c} \right) \quad (16)$$

Bogue and Metzner (13) developed the equations

$$u^+ = 5.57 \log_{10} y^+ + 5.57 - c(\xi, f) \quad (17)$$

$$c(\xi, f) = 0.05 \sqrt{2/f} \exp \frac{-(\xi - 0.8)^2}{0.15} \quad (18)$$

to represent the turbulent core region for Newtonian and non-Newtonian fluids. Popovich and Hummel observed turbulence at all times for values of y^+ greater than 34.6. Thus Equations (17) and (18) at $y^+ = 34.6$ should give an estimate of u_L^+ at the boundary layer of the turbulent core. A value of 14.1 is calculated for the Reynolds number range of 10,000 to 25,000 for a smooth pipe. Figure 1 shows Equations (14) and (16) for $u_L^+ = 14.1$ with experimental data from four references (3, 5, 15, 16). It is observed that this model appears to give an excellent representation of the velocity profile data from $y^+ = 2$ to $y^+ = 34.6$.

DIFFUSIVITY DATA FOR THE TRANSITION REGION

Temperature profile data have been experimentally determined for the region $y^+ = 5$ to $y^+ = 35$ with transfer at constant heat flux. Johnk and Hanratty (17) obtained data for air in a 3.084-in. diam. pipe for the Reynolds number range of 17,700 to 71,200. Gowen and Smith (18) used a 2.058-in. pipe for air, water, and 30% ethylene glycol in water. These data can be used with the Boussinesq equation

$$\epsilon_H/\nu = \frac{\dot{q}_r/\dot{q}_w}{d_t/d_y} - \frac{1}{N_{Pr}} \quad (19)$$

to calculate ϵ_H/ν . The radial correction for Equation (19) can be estimated from Figure 1 of the paper by Smith, Gowen, and Wasmund (19). This represents only a small correction with the wall region. Figure 2 shows these calculated data as a function of y^+ . A line is also shown to represent ϵ_m/ν as obtained from the velocity profile with the equation

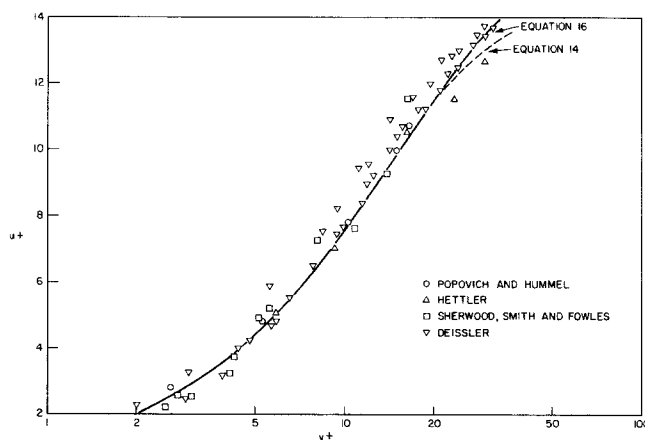


Fig. 1. Velocity profile.

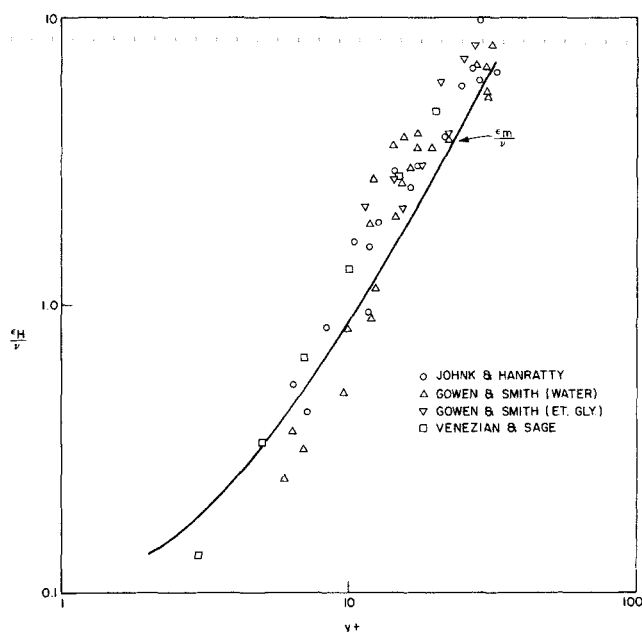


Fig. 2. Eddy diffusivity for the transition region.

$$\epsilon_m/\nu = \frac{1 - y/y_0}{du^+/dy^+} - 1 \quad (20)$$

Reasonable agreement is observed between ϵ_H and ϵ_m . Data for eddy diffusivity of air flowing between two parallel plates are reported by Venezian and Sage (20). Smoothed data points from this work are also shown by Figure 2. Good agreement is observed between these data and the data calculated from the temperature profiles.

EDDY DIFFUSIVITY MODEL—HEAT TRANSFER DATA

Equation (20) was used to represent eddy diffusivity for heat for $y^+ = 2$ to $y^+ = 35$ and to calculate a transfer coefficient for this region. The transfer coefficient for the laminar sublayer could then be estimated from the experimental coefficient and the calculated coefficient for the transition region. Heat transfer data are available from Friend and Metzner (21) for a range of high Prandtl number fluids in a 0.71-in. diam. pipe, from Bernardo and Eian (22) for glycol in a 0.45-in. diam. pipe, Eagle and Ferguson (23) for water in a 1.45-in. diam. pipe, and Dipprey and Sibersky (24) for water in a 0.375-in. pipe. Estimated heat transfer resistance of the transition region was about 20% of the total resistance for the high Prandtl number data and about 50% for the other data. Laminar boundary-layer heat transfer coefficients calculated from these data are shown as the equivalent dimensionless mass transfer coefficients in Figure 3. These data can represent an extrapolation of either Equation (7) or (8). Therefore a single equation eddy diffusivity model is not obvious.

MARCHELLO AND TOOR MODEL

Equation (4) can be used to analyze the data for laminar sublayer coefficients with the assumptions that

1. The term l in Equation (5) represents one-half the boundary-layer thickness.
2. The mean frequency of mixing S can be represented by the frequency data obtained by Shaw and Hanratty for the laminar sublayer. These frequency data represent the local fluctuations in the mass transfer coefficient in a 1-in. pipe for the Reynolds number range of 10,000 to 60,000. The frequency distribution data were analyzed to determine the effective average frequency for mass trans-

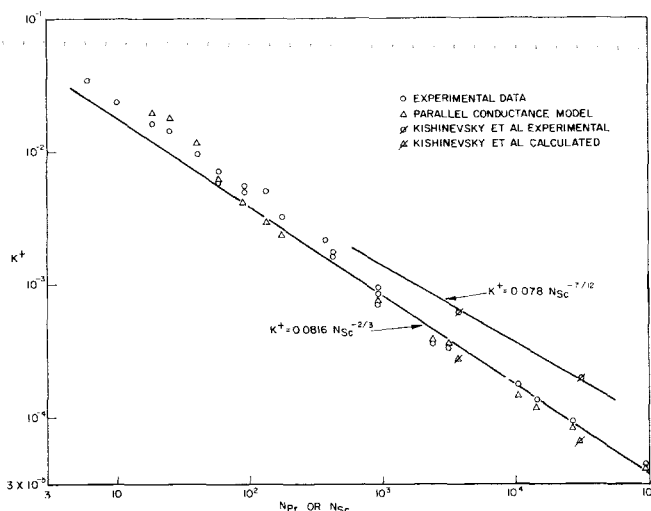


Fig. 3. Model comparison with experimental data.

fer at each Reynolds number. These results are empirically expressed by the equation

$$\frac{1}{S} = \frac{1}{n} = 145/(u^*/\nu)^{0.8} \quad (21)$$

Analysis of the Harriott and Hamilton data showed l to be a function of the Schmidt number rather than a hydrodynamic function.

PARALLEL CONDUCTANCE MODELS

Equation (6) represents this type of model. The Popovich and Hummel observations indicate that the model should be revised to represent the fraction of the total time that corresponds to each of the transport mechanisms.

$$k_E = \alpha k_L + (1 - \alpha) 2 \sqrt{\frac{D}{\pi \theta_c}} \quad (22)$$

Thus α is the fraction of the total time that the laminar condition exists. The laminar coefficient is obtained from the equation for well-developed flow

$$k_L = \frac{u^*}{y_{BL}^+ N_{Sc}} \quad (23)$$

and the time that a fluid element is in contact with the wall is

$$\theta_c = (1 - \alpha)\theta \quad (24)$$

The time θ can be obtained from the empirical representation of the Shaw and Hanratty frequency data, Equation (21).

The observations reported by Popovich and Hummel represent a Reynolds number of 13,100 in a 1-in. sq. pipe. Mass transfer fluctuations reported by Shaw and Hanratty represent a 1-in. pipe. The kinematic viscosity was about 0.064 sq.ft./hr. for both experimental systems. Thus it is of interest to consider mass transfer data with respect to these observations. Assumed numerical values are

1. The laminar sublayer thickness is $y^+ = 2.0$ from the Popovich and Hummel work.
2. Laminar flow exists 55% of the total time as indicated by the Popovich and Hummel data.
3. Empirical Equation (21) represents the time θ for the range of u^{*2}/ν from 3.4×10^6 to 7.9×10^7 hr.⁻¹. These assumptions, with Equations (22), (23), and (24), then provide a test of this model.

Son and Hanratty report corrected average mass transfer coefficients for the Shaw and Hanratty work. A value

of $k^+ = 3.56 \times 10^{-4}$ is reported for a Reynolds number of 11,000. The calculated value with the above assumptions and Equations (22), (23), and (24) is $k^+ = 3.71 \times 10^{-4}$. Shaw and Hanratty report large fluctuations in local values of the coefficient. Frequency data at a Reynolds number of 10,400 shows that the maximum frequency can be about 2 sec.⁻¹. The penetration theory mass transfer coefficient corresponding to this frequency is three times the coefficient for the laminar condition. Thus this model indicates a threefold range in the local coefficient at this specific flow condition. It is also interesting to observe that the assumption of a laminar sublayer thickness of $y^+ = 2.0$ results in an average velocity for the sublayer that is equal to the friction velocity. Shaw and Hanratty estimated disturbance velocities at two Reynolds numbers from their data. These are reported as

Reynolds Number	Disturbance velocity, cm./sec.	Friction velocity, cm./sec.
15,900	4.5	4.6
21,000	6.3	5.6

The assumption used in the model is obviously consistent with these estimates.

Harriott and Hamilton report an average mass transfer coefficient of $k^+ = 3.22 \times 10^{-4}$ for a Reynolds number of 10,000 and $\nu = 0.065$ sq.ft./hr. The calculated value with the assumptions and this model is $k^+ = 3.29 \times 10^{-4}$. The Harriott and Hamilton data represent a range of Schmidt numbers at a Reynolds number of 10,000. The assumptions and the model can be tested with these data. Figure 3 shows a comparison of the experimental and calculated average mass transfer coefficients. The good agreement obtained indicates that these assumptions are valid for a range of Schmidt numbers with a 1-in. pipe at approximately the Reynolds number of the Popovich and Hummel observations and conditions corresponding to the frequency data of Shaw and Hanratty.

Son and Hanratty report average mass transfer coefficients for the Reynolds number range of 7,750 and 50,200 from the Shaw and Hanratty work which indicate that the dimensionless coefficient is essentially constant for this range. The laminar sublayer thickness and time fraction for laminar flow in the sublayer observed at $N_{Re} = 13,100$ would not necessarily be expected to represent the condition at other Reynolds numbers. Values of $y^+ = 2.0$ for the sublayer thickness and $\alpha = 0.55$ with $N_{Re} = 50,200$ yield $k^+ = 3.2 \times 10^{-4}$ for the Shaw and Hanratty conditions. This indicates that either the sublayer thickness must decrease or α must decrease or both with increasing Reynolds number if the model is valid. Harriott and Hamilton report data for Reynolds numbers up to 100,000. These data also indicate the same Reynolds number response as the Shaw and Hanratty data.

The Shaw and Hanratty work provide frequency data for a 1-in. pipe. The heat transfer data used in the eddy diffusivity model analysis can also be used with this model to indicate whether the frequencies in the sublayer are a function of pipe diameter. The heat transfer data at Reynolds numbers of 10,000 to 14,000 and within the u^{*2}/ν range of the Shaw and Hanratty data were used for this analysis. Assumption of $y^+ = 2.0$ for the sublayer thickness and $\alpha = 0.55$ with Equation (21) for the frequency with the conductance model yields the comparison shown by Figure 3. The Kishinevsky et al. mass transfer data for a 0.51-in. pipe are also shown. It is observed that the parallel resistance model gives at least as good agreement as the eddy diffusivity model for the heat transfer data. The Kishinevsky et al. mass transfer data are also higher

than predicted by this model. Therefore it is of interest to compare the oscillation frequency in the sublayer with the frequency at the boundary of the turbulent core and the transition region.

FREQUENCY COMPARISON

The time θ_c can be obtained from Equation (13) with the probability that a fluid mass has been in contact with the wall for a time θ and $\theta + d\theta$ defined as

$$\phi(\theta) d\theta = \frac{d\theta}{\theta_c} \quad (25)$$

and then averaging the effect of all masses in contact with the wall

$$\tau_0 g_c = \int_0^{\theta_c} \rho u_L \sqrt{\frac{\mu}{\rho \pi \theta}} \frac{d\theta}{\theta_c} = 2 \rho u_L \sqrt{\frac{\mu}{\rho \pi \theta_c}} \quad (26)$$

This was shown by Hanratty in the development of Equation (14). Thus from Equation (26)

$$\begin{aligned} u^* &= \sqrt{\tau_0 g_c / \rho} \\ u_L^+ &= u_L / u^* \\ \theta_c &= \frac{4 \nu (u_L^+)^2}{\pi (u^*)^2} \end{aligned} \quad (27)$$

Equation (27) represents the frequency at the turbulent core boundary. Substitution of $u_L^+ = 14.1$ results in the relationship

$$\frac{n\nu}{u^{*2}} = 3.94 \times 10^{-3} \quad (28)$$

This frequency can then be compared with values of the frequency fluctuations for the laminar sublayer. The Shaw and Hanratty data for the sublayer show the dimensionless frequencies:

Reynolds Number	$n\nu/u^{*2}$
10,400	3.3×10^{-4}
27,700	2.3×10^{-4}
60,100	1.28×10^{-4}

Thus the frequencies in the laminar sublayer are 3.3 to 8.4% of the frequency at the turbulent core boundary for a 1-in. pipe. The frequency in the laminar sublayer may then be a function of the pipe diameter because of a distance-damping effect on the core boundary frequency, but this effect is not shown by the heat transfer data for the smaller pipe diameters.

ANALYSIS FOR DEVELOPING FLOW

Ruckenstein (25, 26) has used a developing flow model for the laminar sublayer to obtain a mass transfer equation corresponding to the eddy diffusivity model with $n = 3$. This analysis results in an equation of the form

$$k^+ = b (N_{Sc})^{-2/3}$$

with the constant b obtained from mass transfer data. It is apparent that this is the same as Equation (7) and that $b = 0.0816$ from the Harriott and Hamilton data. The value of b can also be obtained from the laminar layer thickness and the frequency at the turbulent core boundary.

The thickness of the laminar sublayer is very small in comparison to the pipe diameter so the condition is essentially that for a developing boundary layer on a flat plate.

This is represented by Equation (27):

$$k = 0.664 D \left(\frac{\nu}{D} \right)^{1/3} \left(\frac{u_0}{\nu x_0} \right)^{1/2} \quad (29)$$

The velocity at the surface of the laminar boundary layer is

$$u_0 = u^+_{BL} u^* \quad (30)$$

where u^+_{BL} is the dimensionless velocity at this surface. If the time-averaged velocity profile from Figure 1 is used, an average velocity u^+_a can be estimated for the boundary layer. The length for developing flow is the distance traveled by the fluid in the boundary layer between fluctuations from the turbulent exchange of mass and momentum with the wall.

$$x_0 = u^+_a u^* \theta_c \quad (31)$$

Equation (27) provides an estimate of θ_c , so combining Equations (27) and (31)

$$x_0 = \frac{4 u^+_a (u^+_{BL})^2 \nu}{\pi u^*} \quad (32)$$

and then combining Equations (29), (30), and (32)

$$k^+ = 0.664 \left[\frac{\pi u^+_{BL}}{4 u^+_a (u^+_{BL})^2} \right]^{1/2} (N_{Sc})^{-2/3} \quad (33)$$

Popovich and Hummel report a most probable value of $y^+ = 4.3$ for the laminar sublayer thickness. This represents values of $u^+_{BL} = 4$ and $u^+_a = 2.1$. If u^+_{BL} is assumed to be 14.1, Equation (33) reduces to

$$k^+ = 0.057 (N_{Sc})^{-2/3}$$

This is of the same order of magnitude as Equation (7), which represents experimental mass transfer data.

SUMMARY

Consideration of models for the laminar sublayer of turbulent pipe flow indicates that eddy diffusivity and parallel conductance models may be consistent with experimental heat and mass transfer data. The conductance model shows excellent agreement with mass transfer data at the specific conditions observed by Popovich and Hummel for the sublayer and for the fluctuation frequencies obtained by Shaw and Hanratty for the sublayer. An eddy diffusivity model is derived for developing flow in the sublayer with fluctuations from turbulent exchange of mass and momentum with the wall that gives order of magnitude agreement with experimental mass transfer data.

NOTATION

D = molecular diffusion coefficient, sq.ft./hr.
 g_c = conversion constant, (ft.) (lb.m.) / (lb.f.) (hr.²)
 k = mass transfer coefficient, ft./hr.
 k_E = experimental mass transfer coefficient, ft./hr.
 k_L = mass transfer coefficient for laminar flow, ft./hr.
 k^+ = dimensionless mass transfer coefficient, k_E/u^*
 l = one-half width of mixing region in laminar sublayer, ft.
 N_{Pr} = Prandtl number
 N_{Re} = Reynolds number
 N_{Sc} = Schmidt number, ν/D
 n = frequency, hr.⁻¹
 S = mean frequency of mixing in laminar sublayer, hr.⁻¹
 u = velocity in axial direction, ft./hr.
 u^+_a = average dimensionless velocity in sublayer

u_L = velocity in axial direction of fluid mass before contact with the wall, ft./hr.
 u_0 = velocity at surface of sublayer, ft./hr.
 u^+ = u/u^*
 u^* = $\sqrt{\tau_0 g_c / \rho}$
 x_0 = length for developing flow in sublayer, ft.
 y = perpendicular distance from the wall, ft.
 y^+ = $y \sqrt{\tau_0 g_c / \rho} / \nu$
 y_0 = pipe radius, ft.
 β = turbulence parameter
 δ = thickness of laminar sublayer in fully developed laminar flow, ft.
 ϵ = eddy diffusivity, sq.ft./hr.
 θ = time, hr.
 θ_c = total time for which a fluid mass has been in contact with the wall, hr.
 μ = fluid viscosity, lb.m./ (ft.) (hr.)
 ν = kinematic viscosity, μ/ρ , sq.ft./hr.
 ξ = y/y_0
 ρ = fluid density, lb.m./cu.ft.
 τ_0 = shear stress at wall, lb.f./ft.

Subscripts

BL = sublayer
 H = heat
 m = momentum

LITERATURE CITED

1. Fage, A., and H. C. H. Townend, *Proc. Roy. Soc. (London)*, **135**, 656 (1932).
2. Lin, C. S., R. W. Moulton, and G. L. Putnam, *Ind. Eng. Chem.*, **45**, 636 (1953).
3. Popovich, A. T., and R. L. Hummel, *AIChE J.*, **13**, 854 (1967).
4. Son, J. S., and T. J. Hanratty, *ibid.*, **13**, 689 (1967).
5. Sherwood, T. K., K. A. Smith, and P. E. Fowles, *Chem. Eng. Sci.*, **23**, 1225 (1968).
6. Harriott, P., *ibid.*, **17**, 149 (1962).
7. Marchello, J. M., and H. L. Toor, *Ind. Eng. Chem. Fundamentals*, **2**, 8 (1963).
8. Hughmark, G. A., *ibid.*, **8**, 31 (1969).
9. Shaw, P. V., and T. J. Hanratty, *AIChE J.*, **10**, 475 (1964).
10. Harriott, P., and R. M. Hamilton, *Chem. Eng. Sci.*, **20**, 1073 (1965).
11. Hughmark, G. A., *AIChE J.*, **14**, 352 (1968).
12. Kishinevsky, M. K., T. B. Denisova, and V. A. Parmenov, *Intern. J. Heat Mass Transfer*, **9**, 1779 (1966).
13. Hanratty, T. J., *AIChE J.*, **2**, 359 (1956).
14. Bogue, D. C., *Ind. Eng. Chem. Fundamentals*, **2**, 143 (1963).
15. Hettler, J. P., P. Muntzer, and O. Scrivener, *Comp. Rend.*, **258**, 4201 (1964).
16. Deissler, R. G., *Natl. Advisory Comm. Aeronaut. Tech. Note*, 2138 (1950).
17. Johnk, R. E., and T. J. Hanratty, *Chem. Eng. Sci.*, **17**, 867 (1962).
18. Gowen, R. A., and J. W. Smith, *ibid.*, **22**, 1701 (1967).
19. Smith, J. W., R. A. Gowen, and B. O. Wasmund, *Chem. Engr. Progr. Symp. Ser. No. 77*, 63, 92 (1967).
20. Venezian, E., and B. H. Sage, *AIChE J.*, **7**, 688 (1961).
21. Friend, W. L., and A. B. Metzner, *ibid.*, **4**, 393 (1958).
22. Bernardo, E., and C. S. Eian, *Natl. Advisory Comm. Aeronaut. ARR No. E5F07* (1945).
23. Eagle, A., and R. M. Ferguson, *Proc. Roy. Soc. London*, **A127**, 540 (1930).
24. Dipprey, D. F., and R. H. Sabersky, *Intern. J. Heat Mass Transfer*, **6**, 329 (1963).
25. Ruckenstein, E., *Chem. Eng. Sci.*, **18**, 233 (1963).
26. *Ibid.*, **22**, 474 (1967).
27. Pohlhausen, E., *Angew. Math. Mech.*, **1**, 115 (1921).

Manuscript received July 18, 1969; revision received November 4, 1969; paper accepted November 10, 1969. Paper presented at AIChE Washington meeting.